HHS Public Access

Author manuscript

Cell Rep. Author manuscript; available in PMC 2022 August 15.

Published in final edited form as:

Cell Rep. 2022 May 03; 39(5): 110755. doi:10.1016/j.celrep.2022.110755.

A TLR4-independent critical role for CD14 in intracellular LPS sensing

Swathy O. Vasudevan[1], **Ashley J. Russo**[1], **Puja Kumari**[1], **Sivapriya Kailasan Vanaja**[1,*], **Vijay A. Rathinam**[1,2,*]

[1]Department of Immunology, University of Connecticut Health School of Medicine, 263 Farmington Avenue, Farmington, CT 06030, USA

[2]Lead contact

SUMMARY

Intracellular lipopolysaccharide (LPS) sensing by the noncanonical inflammasome comprising caspase-4 or −11 governs antibacterial host defense. How LPS gains intracellular access *in vivo* is largely unknown. Here, we show that CD14—an LPS-binding protein with a well-documented role in TLR4 activation—plays a vital role in intracellular LPS sensing *in vivo*. By generating *Cd14*$^{-/-}$ and *Casp11*$^{-/-}$ mice strains on a *Tlr4*$^{-/-}$ background, we dissociate CD14's known role in TLR4 signaling from its role in caspase-11 activation and show a TLR4-independent role for CD14 in GSDMD activation, pyroptosis, alarmin release, and the lethality driven by cytosolic LPS. Mechanistically, CD14 enables caspase-11 activation by mediating cytosolic localization of LPS in a TLR4-independent manner. Overall, our findings attribute a critical role for CD14 in noncanonical inflammasome sensing of LPS *in vivo* and establish—together with previous literature—CD14 as an essential proximal component of both TLR4-based extracellular and caspase-11-based intracellular LPS surveillance.

Graphical abstract

*Correspondence: kailasanvanaja@uchc.edu (S.K.V.), rathinam@uchc.edu (V.A.R.).

AUTHOR CONTRIBUTIONS

Conceptualization: V.A.R. and S.K.V.; experimental design and manuscript writing: V.A.R., S.K.V., and S.O.V.; experimental investigation and data analysis: S.O.V., A.J.R., and P.K.

SUPPLEMENTAL INFORMATION

Supplemental information can be found online at https://doi.org/10.1016/j.celrep.2022.110755.

DECLARATION OF INTERESTS

Authors declare no competing interests.

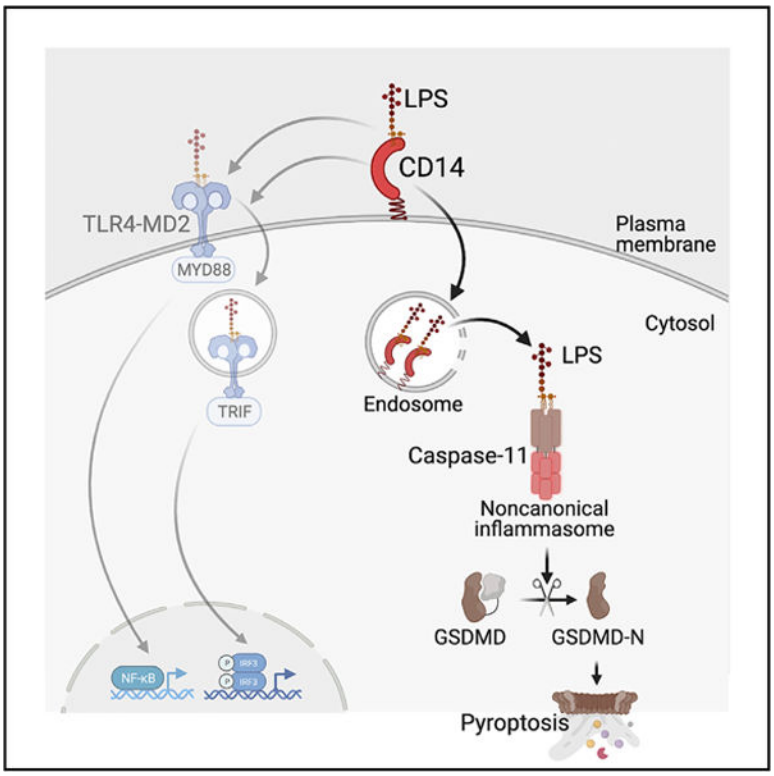

In brief

How LPS attains cytosolic access *in vivo* is unclear. Vasudevan et al. define a TLR4-independent role for CD14 in the cytosolic localization of LPS, triggering noncanonical inflammasome activation and pyroptosis *in vivo*. This finding positions CD14 as an integral component of both extracellular and intracellular LPS surveillance pathways.

INTRODUCTION

Innate immune defense, a frontline host defense strategy, relies on sensing microbial products and activities through an array of germline-encoded pattern recognition receptors (PRRs) (Kawai and Akira, 2010). Upon recognizing microbes, the PRRs initiate signaling cascades involving proteins with scaffolding and enzymatic activities that trigger a wide range of inflammatory and antimicrobial responses contingent in part on the nature of microbial signals and the subcellular sites of their detection. The PRR sensing of microbial products and activities in the cytosol assembles a specialized supramolecular organizing center called inflammasomes (Fitzgerald and Kagan, 2020). The canonical forms of inflammasomes have a receptor such as a nucleotide-binding domain and leucine-rich-repeat-containing (NLR) protein or an absent in melanoma (AIM2)-like receptor (ALR) protein, an adaptor protein (apoptosis-associated speck-like protein containing a CARD, ASC), and an effector molecule, procaspase-1. Inflammasomes convert procaspase-1 into biologically active caspase-1, which subsequently cleaves and activates proinflammatory cytokines IL-1β and IL-18 (Mathur et al., 2017). Caspase-1 also activates a pore-forming protein called gasdermin D (GSDMD) by liberating its N-terminal domain from the

inhibitory C-terminal domain leading to a lytic form of cell death, pyroptosis (Chen et al., 2016; Kayagaki et al., 2015; Liu et al., 2016; Shi et al., 2015).

In contrast to the receptor-adaptor-caspase-1 organization in canonical inflammasomes, a recently discovered noncanonical inflammasome has inflammatory caspases (caspase-11 in rodents and caspase-4 and −5 in humans) functioning as PRRs for intracellular lipopolysaccharide (LPS), a major constituent of Gram-negative bacterial outer membrane (Hagar et al., 2013; Kayagaki et al., 2013; Shi et al., 2014). Direct binding of lipid A of LPS triggers oligomerization and activation of caspase-11, −4, and −5, leading to GSDMD processing and pyroptosis. Furthermore, the membrane disruption by GSDMD's N-terminal fragment (GSDMD-N) leads to the activation of the NLRP3 inflammasome and the maturation of caspase-1, IL-1β, and IL-18 (Kayagaki et al., 2015; Rühl and Broz, 2015; Schmid-Burgk et al., 2015). The pyroptotic cell death and the concomitant release of proinflammatory mediators, including IL-1 cytokines and alarmins, are considered to play important roles in Gram-negative bacterial infections and septic shock (Kayagaki et al., 2011; Rathinam et al., 2019; Russo et al., 2021; Wang et al., 1999).

A poorly understood aspect of the noncanonical inflammasome pathway is the molecular basis of cytosolic access of LPS. Purified LPS lacks the ability to cross biological membranes to reach the cytosol of cells *in vitro* (Vanaja et al., 2016). However, during infections, LPS associated with bacteria or outer membrane vesicles (OMVs) secreted by bacteria gains access to the host cell cytosol (Vanaja et al., 2016). In contrast, free LPS shed from bacteria or even purified LPS can access the cytosol and activate caspase-11 uniquely *in vivo* but not *in vitro* (Kayagaki et al., 2013; Vanaja et al., 2016). HMGB1, a damage-associated molecular pattern (DAMP) with a capacity to bind LPS, has been shown to be involved in the intracellular transport of LPS (Deng et al., 2018; Kim and Kim, 2018). Nonetheless, the mechanisms by which free LPS translocates into the cytosol and activates the noncanonical inflammasome *in vivo* mostly remain elusive.

CD14 is a glycophosphatidylinositol-anchored plasma membrane protein and has a long-established role in LPS-mediated TLR4 activation; CD14 binds and transfers LPS to the TLR4-MD2 complex initiating the myddosome assembly and signal transduction (Dagvadorj et al., 2015; Ferrero et al., 1993; Gutsmann et al., 2001; Haziot et al., 1995, 1996; Latz et al., 2002; Moore et al., 2000; Perera et al., 1997; Schromm et al., 1996; Tan et al., 2015; Wright et al., 1990; Youn et al., 2008). Furthermore, CD14 promotes MD2-dependent TLR4 internalization into endosomes, where TLR4 engages TRIF-TRAF3 signaling to stimulate IRF3-dependent type I interferon expression (Kagan et al., 2008; Zanoni et al., 2011). Whereas the role of CD14 in TLR4-mediated host responses to LPS is well characterized, its role in noncanonical inflammasome sensing of cytosolic LPS is unknown. By generating *Cd14*$^{-/-}$ mice on a *Tlr4*-deficient background, we reveal that CD14 plays an essential TLR4-independent role in caspase-11 activation *in vivo* by delivering LPS intracellularly. Thus, we demonstrate CD14 as an integral component of the noncanonical inflammasome *in vivo*.

RESULTS

Noncanonical inflammasome activation by LPS *in vivo* is CD14-dependent

To investigate the role of CD14 in noncanonical inflammasome activation, we injected wild-type and *Cd14*$^{-/-}$ mice with LPS and measured plasma IL-1β and IL-18. CD14 is necessary for TLR4 activation of TRIF signaling and type I interferons (Zanoni et al., 2011), which prime the noncanonical inflammasome by upregulating caspase-11 expression (Rathinam et al., 2012). Therefore, to ensure that the priming step is not compromised in *Cd14*$^{-/-}$ mice, mice were first injected with IFN-γ. IFN-γ priming obviates TLR4-dependent priming of the noncanonical inflammasome, and as a result, caspase-11-mediated responses such as GSDMD activation and IL-18 secretion to cytosolic LPS are intact in IFN-γ-primed *Tlr4*$^{-/-}$ mice (Figures 1A and 1B). IL-1β release was, however, reduced in IFN-γ-primed and LPS-injected *Tlr4*$^{-/-}$ mice (Figure S1A), which is most likely due to impaired proIL-1β transcription. Importantly, all these noncanonical inflammasome responses, but not TNF, were abolished in IFN-γ-primed *Casp11*$^{-/-}$ mice, reinforcing the TLR4-independent intracellular sensing of LPS by caspase-11 (Figures 1A, 1B, and S1B).

Notably, IFN-γ-primed *Cd14*$^{-/-}$ mice displayed tremendously impaired noncanonical inflammasome responses to LPS characterized by a minimal secretion of IL-18 and IL-1β into the plasma (Figures 1C and 1D). Furthermore, cytosolic LPS-induced GSDMD activation was also significantly reduced in the spleens of IFN-γ-primed *Cd14*$^{-/-}$ mice compared with IFN-γ-primed wild-type mice (Figure 1E). Thus, *Cd14*$^{-/-}$ mice phenocopied *Casp11*$^{-/-}$ mice with respect to host responses to intracellular LPS. Moreover, IFN-γ-primed *Cd14*$^{-/-}$ mice were highly resistant to endotoxic shock (Figures 1F and 1G). Splenic caspase-11, GSDMD, and NLRP3 expression was comparable between IFN-γ-primed wild-type and *Cd14*$^{-/-}$ mice (Figure 1E). Taken together, these data indicate that CD14 is necessary for mediating noncanonical inflammasome responses to LPS *in vivo* and that poor noncanonical inflammasome responses in *Cd14*$^{-/-}$ mice are not due to an inherent priming issue but rather due to impaired caspase-11 activation.

CD14 functions independent of TLR4 to activate the noncanonical inflammasome

Given CD14's significant roles in TLR4 signaling, we next sought to determine if CD14 functions independent of TLR4 in noncanonical inflammasome activation. To examine CD14's role in a TLR4-deficient experimental system, we generated *Tlr4*$^{-/-}$ *Cd14*$^{-/-}$ mice by crossing *Tlr4*$^{-/-}$ mice and *Cd14*$^{-/-}$ mice. Additionally, we made *Tlr4*$^{-/-}$ *Casp11*$^{-/-}$ mice for comparison purposes by crossing *Tlr4*$^{-/-}$ mice and *Casp11*$^{-/-}$ mice. *Tlr4*$^{-/-}$, *Tlr4*$^{-/-}$ *Cd14*$^{-/-}$, and *Tlr4*$^{-/-}$ *Casp11*$^{-/-}$ mice were primed with IFN-γ and administered with LPS; *Tlr4*$^{-/-}$ mice displayed a robust noncanonical inflammasome activation evident from GSDMD processing in the spleen and IL-1β and IL-18 secretion into the plasma (Figures 2A–2F), confirming TLR4-independent activation of the noncanonical inflammasome. In contrast, *Tlr4*$^{-/-}$ *Cd14*$^{-/-}$ mice, like *Tlr4*$^{-/-}$ *Casp11*$^{-/-}$ mice, failed to mount IL-1β and IL-18 responses to LPS (Figures 2A, 2B, 2D, and 2E). In addition, GSDMD cleavage was also significantly reduced in *Tlr4*$^{-/-}$ *Cd14*$^{-/-}$ and *Tlr4*$^{-/-}$ *Casp11*$^{-/-}$ mice compared with *Tlr4*$^{-/-}$ mice (Figures 2C and 2F), whereas splenic caspase-11, GSDMD, and NLRP3 expression was comparable. Similarly, cytosolic LPS-induced release of DAMPs such as

IL-1α and the recently identified galectin-1 (Russo et al., 2021) was also reduced in *Tlr4*$^{-/-}$ *Cd14*$^{-/-}$ mice compared with *Tlr4*$^{-/-}$ mice (Figures 2G, 2H, and 2I).

Furthermore, IFN-γ-primed *Tlr4*$^{-/-}$ mice succumbed to the LPS challenge, whereas IFN-γ-primed *Tlr4*$^{-/-}$ *Cd14*$^{-/-}$ and *Tlr4*$^{-/-}$ *Casp11*$^{-/-}$ mice were almost completely resistant (Figures 3A and 3B). In line with the improved survival, *Tlr4*$^{-/-}$ *Cd14*$^{-/-}$ mice were also significantly protected from hypothermia (Figure 3C) and vascular coagulopathy, which is evident from their lower plasma levels of tissue factor-3 and prothrombin time (Figures 3D and 3E). It is clear from these data that the TLR4-independent function of CD14 is necessary for cytosolic LPS-elicited caspase-11 activation and pathophysiological manifestations. Notably, data from *Tlr4*$^{-/-}$ *Cd14*$^{-/-}$ mice provide solid genetic evidence that CD14's roles in TLR4 and caspase-11 pathways are separable.

CD14 enables caspase-11 activation by facilitating intracellular LPS localization in a TLR4-independent manner

Having established the TLR4-independent role of CD14 in caspase-11-mediated endotoxic shock, we next sought to identify the mechanism underlying CD14's role in noncanonical inflammasome activation. Considering that CD14 is known to bind LPS and endogenous lipids such as oxPAPC and induce their internalization as well as that of TLR4 (Dagvadorj et al., 2015; Kitchens and Munford, 1998; Luchi and Munford, 1993; Zanoni et al., 2011, 2017), we hypothesized that CD14 mediates caspase-11 activation by mediating cytosolic translocation of LPS. To examine this, we injected mice with LPS and measured LPS quantity in the cytosol of splenic myeloid cells—which we identified as a primary cell type involved in cytosolic LPS sensing *in vivo* (Kumari et al., 2021)—using the HEK-Blue TLR4 reporter cell and the standard limulus amebocyte lysate (LAL) assays. The cytosol was extracted from CD11b^{+} myeloid cells, sorted from the spleen, using a digitonin-based fractionation method that we optimized previously to assess cytosolic LPS (Vanaja et al., 2016). We found that cytosolic LPS levels, as revealed by the HEK-Blue TLR4 reporter and LAL assays, were comparable between wild-type and *Tlr4*$^{-/-}$ myeloid cells (Figures 4A and 4B). In contrast, the cytosol of splenic myeloid cells from *Tlr4*$^{-/-}$ *Cd14*$^{-/-}$ mice contained little LPS (Figures 4A and 4B).

To further test our hypothesis, we used confocal microscopy to visualize intracellular LPS. Control and mutant mice were injected with FITC-LPS, or unlabeled LPS as control, and the LPS localization was tracked in CD11b^{+} myeloid cells sorted from the spleen. FITC-LPS colocalized with CD14 on the cell surface and in the intracellular space (Figure S2A). Furthermore, FITC-LPS was visualized in early endosomes, lysosomes, and nonlysosomal compartments (Figure S2B). Importantly, intracellular FITC-LPS was visualized in *Tlr4*$^{-/-}$ cells but not in *Tlr4*$^{-/-}$ *Cd14*$^{-/-}$ cells (Figures 4C, 4D, and 4E). Quantification of intracellular FITC intensity confirmed that *Tlr4*$^{-/-}$ *Cd14*$^{-/-}$ cells have significantly reduced intracellular LPS (Figure 4F). We next used electron microscopy (EM) to better visualize cytosolic localization of LPS; peritoneal lavage cells from FITC-LPS-injected or unlabeled LPS-injected (as control) mice were subjected to staining with gold-conjugated anti-FITC antibody followed by EM imaging. The cytosolic localization of LPS—indicated by intracellular LPS staining outside organelle structures— was visible

in cells from FITC-LPS-injected wild-type and *Tlr4*$^{-/-}$ mice but not *Tlr4*$^{-/-}$ *Cd14*$^{-/-}$ mice (Figure 4G). These data reinforce the role of CD14 in the cytosolic translocation of LPS. These data collectively indicate that CD14 mediates LPS internalization into the cytosol *in vivo* independently of TLR4. In line with this finding, the introduction of LPS into the cytosol of BMDMs by transfection bypasses the requirement for CD14 and activates pyroptosis and IL-1β secretion in a CD14-independent manner (Figure S2C).

Since HMGB1 has been shown to mediate LPS uptake and release into the cytosol, we tested if CD14 plays a role in this process. Whereas the BMDM uptake of LPS was poor, which could be attributed to the low dose of LPS used, we found that the BMDM internalization of LPS complexed with HMGB1 occurred in a CD14-independent but receptor for advanced glycation end-products (RAGE)-dependent manner (Figure S3). Finally, to understand how LPS internalized via CD14 eventually translocates into the cytosol, we tested if CD14-mediated uptake of LPS results in early endosomal disruption, which perhaps is sufficient for LPS to gain access to the cytosol. For this, we assessed the early endosomal localization of galectin-3 (a sensor of endomembrane damage) as a proxy for the loss of endosomal integrity (Canton et al., 2020; Paz et al., 2010). We observed galectin-3 recruitment to Rab5+ early endosomes in splenic myeloid cells from LPS-injected wild-type and *Tlr4*$^{-/-}$ mice but not *Tlr4*$^{-/-}$ *Cd14*$^{-/-}$ mice (Figure S4). These data lend evidence to the idea that the endolysosomal membrane permeabilization occurring upon CD14-dependent LPS uptake may underlie the cytosolic access of LPS as it has been proposed for HMGB1-mediated delivery of LPS (Deng et al., 2018).

DISCUSSION

Intracellular sensing of microbial products dictates critical host defense responses during infections (Wright et al., 2021). The noncanonical inflammasome—via caspase-11 in mice and caspase-4 in humans—senses bacterial LPS that gains access to the cytosol and triggers inflammatory responses characterized by pyroptosis (Hagar et al., 2013; Kayagaki et al., 2013; Shi et al., 2014). Here, we identify CD14 as an essential component of the intracellular LPS sensing pathway *in vivo*. We found that CD14 facilitates the intracellular localization of LPS and caspase-11 activation *in vivo*. Using *Tlr4*$^{-/-}$ *Cd14*$^{-/-}$ mice, we show that the role of CD14 in intracellular LPS sensing is separable from its known role in TLR4 signaling. Given that pathological inflammation mediated by caspase-11 is linked to sepsis in murine models (Cheng et al., 2017; Kayagaki et al., 2011; Kumari et al., 2021; Russo et al., 2021), the specific role of CD14 in facilitating intracellular LPS sensing and noncanonical inflammasome activation reported in this study likely contributes to CD14's detrimental effects in endotoxemia.

Though CD14 has been known to mediate LPS internalization (Dagvadorj et al., 2015; Kitchens and Munford, 1998; Luchi and Munford, 1993), its biological relevance—particularly in the context of caspase-11-dependent intracellular LPS sensing—is not known. Our data show that LPS internalization via CD14 is a consequential event that enables cytosolic translocation of LPS, licensing pyroptotic and IL-1 responses from the host. Furthermore, it has been shown that CD14 captures endogenous lipid DAMPs, such as oxPAPC, in the extracellular space and transports them into endosomes, leading to

inflammasome activation and hyperactivation of dendritic cells (Zanoni et al., 2017). Thus, the capacity to directly capture lipids of host and microbial origins and trigger their internalization (Dagvadorj et al., 2015; Kitchens and Munford, 1998; Luchi and Munford, 1993; Zanoni et al., 2011, 2017) makes CD14 highly relevant in the context of cytosolic immune surveillance.

Following CD14-mediated internalization, LPS is visualized in EEA1+ early endocytic compartments in this study. We have previously shown that LPS associated with bacterial OMVs traffics to early endosomes from where it gains access to the cytosol (Vanaja et al., 2016). Considering that LPS trafficking to early endosomes favors its cytosolic translocation (Vanaja et al., 2016), CD14-mediated internalization likely traffics LPS into an early endosomal compartment that permits LPS translocation into the cytosol *in vivo*. Furthermore, the early endosomal membrane disruption, evident from early endosomal accumulation of galectin-3, occurring following CD14-mediated internalization of LPS is perhaps sufficient for its luminal contents such as LPS to be exposed to the cytosol. Supporting this possibility, it has been recently shown that following RAGE-mediated internalization, HMGB1-complexed LPS becomes cytosolic owing to the destabilization of lysosomes by HMBG1 (Deng et al., 2018; Kim and Kim, 2018).

Limitations of the study

While this study has revealed the TLR4-independent contribution of CD14 to caspase-11 activation, it has a few limitations. First, CD14's role is likely to be limited to transporting LPS to early endosomes, and the precise mechanism underlying how LPS translocates from early endosomes to the cytosol following CD14-mediated uptake was not identified in this study. While this study observed CD14-dependent endosomal membrane disruption following LPS internalization, whether this is responsible for the endosomal escape of LPS was not examined. Furthermore, while our experiments show no role for CD14 in HMGB1-mediated internalization of LPS *in vitro*, this work did not determine whether this is also the case *in vivo*. Moreover, the CD14-mediated cytosolic delivery of LPS demonstrated in this study occurs only *in vivo* but not in BMDMs *in vitro* despite the expression of CD14 by BMDMs, which implicates the involvement of a yet-to-be-identifi *in vivo*-specific factor in this event. Another limitation is that our studies are done in the murine model, and we have not evaluated the role of CD14 in promoting LPS internalization and noncanonical inflammasome activation in humans.

STAR★METHODS

RESOURCE AVAILABILITY

Lead contact—Further information and requests regarding resources and reagents can be directed to Vijay Rathinam (rathinam@uchc.edu).

Materials availability—Mouse lines generated in this study are available from the lead contact upon request (subject to their availability at the time of request).

Data and code availability

- All data reported in the paper are available from the lead contact upon request.
- This paper does not report original code.
- Any additional information required to reanalyze the data reported in this paper is available from the lead contact upon request.

EXPERIMENTAL MODEL AND SUBJECT DETAILS

Mice—C57BL/6J, *Cd14*$^{-/-}$, and *Tlr4*$^{-/-}$ mice from the Jackson Laboratory (Bar Harbor, ME) and *Casp11*$^{-/-}$ mice (a kind gift of Dr. Vishva Dixit) were bred and maintained in specific pathogen-free conditions in the animal facility of UConn Health. *Tlr4*$^{-/-}$ *Casp11*$^{-/-}$ and *Tlr4*$^{-/-}$ *Cd14*$^{-/-}$ mice were generated by breeding the respective single KO mice with *Tlr4*$^{-/-}$ mice. Genetic ablation of *Tlr4*, *Cd14*, and *Casp11* was confirmed by PCR analysis of tail genomic DNA. Eight–24-week-old male and female mice were used. All experiments were carried out in accordance with the guidelines set forth by the UConn Health Institutional Animal Care and Use Committee.

Cell culture—Primary BMDMs were generated as described previously (Russo et al., 2021). TLR4-expressing HEK293 cells (HEK-Blue hTLR4; InvivoGen) were cultured in complete DMEM supplemented with 10% FBS and HEK-Blue selection (InvivoGen).

METHOD DETAILS

***In vivo* LPS challenge and cytokine analysis—**Age- and sex-matched C57BL/6J, *Cd14*$^{-/-}$, *Tlr4*$^{-/-}$, *Casp11*$^{-/-}$, *Tlr4*$^{-/-}$ *Casp11*$^{-/-}$, and *Tlr4*$^{-/-}$ *Cd14*$^{-/-}$ mice were injected intraperitoneally (i.p.) with recombinant mouse IFN-γ (1 μg; R&D Systems) for 3 h, followed by 20 or 25 mg/kg of *E. coli* O 111:B4 LPS (Sigma) unless otherwise indicated. Body temperature and survival were monitored for indicated periods. Plasma was collected at 6 h or 18 h post-LPS injection for cytokine analysis. IL-1β, IL-1α, and TNF levels in the plasma were assessed by using appropriate ELISA kits (ThermoFisher). IL-18 was measured by ELISA as previously described (Kumari et al., 2021). Galectin-1 levels were assessed with the DuoSet ELISA kit (R&D Systems) according to the manufacturer's protocol.

Immunoblotting—Spleen lysates were prepared by homogenizing spleen in PBS with protease inhibitor cocktail (Invitrogen). BCA assay was performed to measure protein concentration. Protein (25 μg) was mixed with NuPAGE sample buffer and separated by SDS-PAGE. Samples were transferred to nitrocellulose membrane using Trans-Blot Turbo Transfer System (Bio-Rad) and blocked with 2.5% milk. The membrane was probed with antibodies for mouse GSDMD (clone EPR19828; Abcam catalog no. ab209845), mouse caspase-11 (clone 17D9; Cell Signaling Technology catalog no. 14340) and NLRP3 (clone D4D8T; Cell Signaling Technology catalog no. 15101).

Tissue Factor-III assay and prothrombin time (PT)—Tissue Factor-III in the plasma was assessed by DuoSet Mouse Coagulation Factor III/TF ELISA kit (R&D systems). Prothrombin time was measured using Pacific Hemostasis Thromboplastin-D (Thermo Scientific) according to the manufacturer's instructions (Wu et al., 2019; Yang et al., 2019).

Briefly, blood was collected by cardiac puncture in 3.8% trisodium citrate (1:10 ratio) as an anticoagulant. Plasma was collected by centrifugation and prothrombin time was measured manually by rapidly adding pre-warmed thromboplastin-D to the plasma.

Cytosol fractionation and LPS assessment—Cytosolic fraction was isolated as previously described (Vanaja et al., 2016). Spleens were collected 5 h post-LPS injection and crushed through 100 μm nylon-mesh strainer. RBCs were lysed using ACK lysis buffer (Gibco). Splenocytes were incubated with Fc block, stained with mouse CD11b antibody (Clone M1/70; BioLegend catalog no. 101212) and sorted on BD FACS Aria II. Sorted CD11b + cells were resuspended in 0.001% digitonin buffer for 8 min and supernatant containing the cytosolic content was collected. Cytosolic LPS was quantified using the Limulus Amebocyte Lysate (LAL) assay (Associates of Cape Cod) according to the manufacturer's instructions. HEK293 cells expressing hTLR4 (Invivogen) were cultured with HEK-Blue Detection and HEK-Blue Selection (Invivogen) in a 96-well plate according to the manufacturer's protocol. Cytosol from CD11b+ splenocytes was added to the cell culture medium and SEAP activity was assessed by measuring absorbance at 620–655 nm.

Confocal microscopy—Mice were injected with FITC-conjugated or unlabeled LPS (25 mg/kg) from *E. coli* O111:B4 (Sigma). Spleen was dissected 5 h post-LPS injection and splenocytes were isolated by collagenase digestion with DNase I in BSS at 37°C for 20 min. Splenocytes were crushed through 100 μm nylon-mesh strainer and RBCs were lysed using ACK lysis buffer. Cytospins of CD11b+ splenocytes were fixed with 4% paraformaldehyde and permeabilized with 0.1% Triton-X. Slides were blocked with 10% goat serum and stained with fluorophore-conjugated antibodies against FITC (Clone 1F8.1E4; Biotium catalog no. 20210) and mouse CD45 (Clone 104; Invitrogen catalog no. 17–0454-82). Staining with an anti-FITC antibody was performed to enhance FITC signal, which otherwise might be difficult to detect *in vivo*. Furthermore, immunofluorescence staining was also done as indicated with anti-EEA1 (Clone C45B10; Cell signaling catalog no. 3288S), anti-Lamp1 (Clone eBio1D4B; eBioscience catalog no. 14–1071-85), APC-labeled anti-mouse CD14 (Clone Sa2–8; Invitrogen catalog no. 17–0141-81), anti-galectin-3 (Clone D4I2R; Cell Signaling catalog no. 12733) and anti-Rab5A (Clone E6N8S; Cell Signaling catalog no. 46449S) antibodies and the respective fluorophore-conjugated secondary antibodies. Cells were visualized using Zeiss LSM880 microscope and the intracellular FITC fluorescence was quantified by measuring integrated density of FITC signal normalized to background signal using ImageJ (Parry and Hemstreet, 1988).

BMDM stimulation and staining—To assess cell death and IL-1β secretion, cells were primed with IFN-γ (10 ng/mL; R&D Systems) and Pam3CSK4 (0.5 μg/mL; InvivoGen) for 3 h and stimulated with 1 μg LPS or transfected with LPS (1 μg)-Lipofectamine 2000 (Invitrogen). Supernatants were collected 16 h post-stimulation and cell death was measured by LDH release. IL-1β levels in the supernatant was measured by ELISA. To visualize LPS internalization, BMDMs were stimulated with FITC-LPS (100 ng/mL) or FITC-LPS pre-incubated with recombinant HMGB1 (400 ng/mL) for 20 min at room temperature as described previously (Deng et al., 2018). RAGE-mediated FITC-LPS internalization was assessed by treating BMDMs with DMSO or RAGE inhibitors (1 μM FPS-ZM1

(Cayman), or 10 μM RAGE antagonist peptide (RAP; Millipore) (Deng et al., 2018; Senatus et al., 2020)) 1 h before LPS treatment. Cells were washed with PBS 2 h later, fixed, permeabilized, and blocked as described above and stained with antibodies against FITC and CD45.

Transmission electron microscopy—Peritoneal lavage cells were collected 5 h post FITC-conjugated or unlabeled LPS (25 mg/kg) injection. Cells were plated on 35 mm confocal dish and fixed with 4% paraformaldehyde, followed by blocking and permeabilization with 0.1% saponin in 5% goat serum. To visualize cytosolic LPS, anti-FITC antibody conjugated with nanogold (Electron microscopy science catalog no. 25581) was used. After fixation with 2% glutaraldehyde and the gold particle size was augmented using GoldEnhance EM kit (Nanoprobes) to enhance visualization of gold labelled FITC particle. To obtain a high contrast and image organelles distinctly, cells were stained with 1% osmium tetroxide for 30 min, followed by 1% uranyl acetate staining for 30 min. The samples were then dehydrated and embedded on resin. Ultrathin sections were cut and imaged on a Hitachi H-7650 Transmission Electron Microscope.

QUANTIFICATION AND STATISTICAL ANALYSIS

Statistical analysis was performed on GraphPad Prism using unpaired two-tailed t test, one-way ANOVA, two-way ANOVA, or Mantel-cox test as indicated in the figure legends.

Supplementary Material

Refer to Web version on PubMed Central for supplementary material.

ACKNOWLEDGMENTS

We thank V. Dixit and K. Fitzgerald for *Casp11*$^{-/-}$ mice and N. Frank for the HEK-Blue TLR4 reporter cell line. This work was supported by the NIH (AI119015 and AI148491 to V.R. and AI132850 to S.K.V.).

REFERENCES

Canton J, Blees H, Henry CM, Buck MD, Schulz O, Rogers NC, Childs E, Zelenay S, Rhys H, Domart M-C, et al. (2020). The receptor DNGR-1 signals for phagosomal rupture to promote cross-presentation of dead-cell-associated antigens. Nat. Immunol, 1–14. [PubMed: 31831887]

Chen X, He W-T, Hu L, Li J, Fang Y, Wang X, Xu X, Wang Z, Huang K, and Han J (2016). Pyroptosis is driven by non-selective gasdermin-D pore and its morphology is different from MLKL channel-mediated necroptosis. Cell Res 26, 1007.1020.

Cheng KT, Xiong S, Ye Z, Hong Z, Di A, Tsang KM, Gao X, An S, Mittal M, Vogel SM, et al. (2017). Caspase-11–mediated endothelial pyroptosis underlies endotoxemia-induced lung injury. J. Clin. Invest 127, 4124–4135. [PubMed: 28990935]

Dagvadorj J, Shimada K, Chen S, Jones HD, Tumurkhuu G, Zhang W, Wawrowsky KA, Crother TR, and Arditi M (2015). Lipopolysaccharide induces alveolar macrophage necrosis via CD14 and the P2X7 receptor leading to interleukin-1a release. Immunity 42, 640–653. [PubMed: 25862090]

Deng M, Tang Y, Li W, Wang X, Zhang R, Zhang X, Zhao X, Liu J, Tang C, Liu Z, et al. (2018). The endotoxin delivery protein HMGB1 mediates caspase-11-dependent lethality in sepsis. Immunity 49, 740–753.e7. [PubMed: 30314759]

Ferrero E, Jiao D, Tsuberi BZ, Tesio L, Rong GW, Haziot A, and Goyert SM (1993). Transgenic mice expressing human CD14 Are hypersensitive to lipopolysaccharide. Proc. Nat. Acad. Sci. U S A, 2380–2384.

Fitzgerald KA, and Kagan JC (2020). Toll-like receptors and the control of immunity. Cell 180, 1044–1066. [PubMed: 32164908]

Gutsmann T, Müller M, Carroll SF, MacKenzie RC, Wiese A, and Seydel U (2001). Dual role of lipopolysaccharide (LPS)-Binding protein in neutralization of LPS and enhancement of LPS-induced activation of mononuclear cells. Infect. Immun 69, 6942–6950. [PubMed: 11598069]

Hagar JA, Powell DA, Aachoui Y, Ernst RK, and Miao EA (2013). Cytoplasmic LPS activates caspase-11: implications in TLR4-independent endotoxic shock. Science 341, 1250–1253. [PubMed: 24031018]

Haziot A, Rong GW, Lin XY, Silver J, and Goyert SM (1995). Recombinant soluble CD14 prevents mortality in mice treated with endotoxin (lipopolysaccharide). J. Immunol. Baltim Md 1950 154, 6529–6532.

Haziot A, Ferrero E, Köntgen F, Hijiya N, Yamamoto S, Silver J, Stewart CL, and Goyert SM (1996). Resistance to endotoxin shock and reduced dissemination of gram-negative bacteria in CD14-deficient mice. Immunity 4, 407–414. [PubMed: 8612135]

Kagan JC, Su T, Horng T, Chow A, Akira S, and Medzhitov R (2008). TRAM couples endocytosis of Toll-like receptor 4 to the induction of interferon-b. Nat. Immunol 9, 361–368. [PubMed: 18297073]

Kawai T, and Akira S (2010). The role of pattern-recognition receptors in innate immunity: update on Toll-like receptors. Nat. Immunol 11, 373–384. [PubMed: 20404851]

Kayagaki N, Warming S, Lamkanfi M, Walle LV, Louie S, Dong J, Newton K, Qu Y, Liu J, Heldens S, et al. (2011). Non-canonical inflammasome activation targets caspase-11. Nature 479, 117. [PubMed: 22002608]

Kayagaki N, Wong MT, Stowe IB, Ramani SR, Gonzalez LC, Akashi-Takamura S, Miyake K, Zhang J, Lee WP, Muszyński A, et al. (2013). Noncanonical inflammasome activation by intracellular LPS independent of TLR4. Science 341, 1246–1249. [PubMed: 23887873]

Kayagaki N, Stowe IB, Lee BL, O'Rourke K, Anderson K, Warming S, Cuellar T, Haley B, Roose-Girma M, Phung QT, et al. (2015). Caspase-11 cleaves gasdermin D for non-canonical inflammasome signalling. Nature 526, 666–671. [PubMed: 26375259]

Kim HM, and Kim Y-M (2018). HMGB1: LPS delivery vehicle for caspase-11-mediated pyroptosis. Immunity 49, 582–584. [PubMed: 30332623]

Kitchens RL, and Munford RS (1998). CD14-dependent internalization of bacterial lipopolysaccharide (LPS) is strongly influenced by LPS aggregation but not by cellular responses to LPS. J. Immunol 160, 1920–1928. [PubMed: 9469454]

Kumari P, Russo AJ, Wright SS, Muthupalani S, and Rathinam VA (2021). Hierarchical cell-type-specific functions of caspase-11 in LPS shock and antibacterial host defense. Cell Rep 35, 109012. [PubMed: 33882312]

Latz E, Visintin A, Lien E, Fitzgerald KA, Monks BG, Kurt-Jones EA, Golenbock DT, and Espevik T (2002). Lipopolysaccharide rapidly traffics to and from the golgi apparatus with the toll-like receptor 4-MD-2-CD14 complex in a process that is distinct from the initiation of signal transduction. J. Biol. Chem 277, 47834–47843. [PubMed: 12324469]

Liu X, Zhang Z, Ruan J, Pan Y, Magupalli VG, Wu H, and Lieberman J (2016). Inflammasome-activated gasdermin D causes pyroptosis by forming membrane pores. Nature 535, 153–158. [PubMed: 27383986]

Luchi M, and Munford RS (1993). Binding, internalization, and deacylation of bacterial lipopolysaccharide by human neutrophils. J. Immunol 151, 959–969. [PubMed: 7687625]

Mathur A, Hayward JA, and Man SM (2017). Molecular mechanisms of inflammasome signaling. J. Leukoc. Biol 103, 233–257. [PubMed: 28855232]

Moore KJ, Andersson LP, Ingalls RR, Monks BG, Li R, Arnaout MA, Golenbock DT, and Freeman MW (2000). Divergent response to LPS and bacteria in CD14-deficient murine macrophages. J. Immunol 165, 4272–4280. [PubMed: 11035061]

Parry WL, and Hemstreet GP (1988). Cancer detection by quantitative fluorescence image analysis. J. Urol 139, 270–274. [PubMed: 3339723]

Paz I, Sachse M, Dupont N, Mounier J, Cederfur C, Enninga J, Leffler H, Poirier F, Prevost M, Lafont F, et al. (2010). Galectin-3, a marker for vacuole lysis by invasive pathogens. Cell Microbiol 12, 530–544. [PubMed: 19951367]

Perera PY, Vogel SN, Detore GR, Haziot A, and Goyert SM (1997). CD14-dependent and CD14-independent signaling pathways in murine macrophages from normal and CD14 knockout mice stimulated with lipopolysaccharide or taxol. J. Immunol 158, 4422–4429. [PubMed: 9127007]

Rathinam VAK, Vanaja SK, Waggoner L, Sokolovska A, Becker C, Stuart LM, Leong JM, and Fitzgerald KA (2012). TRIF licenses caspase-11-dependent NLRP3 inflammasome activation by gram-negative bacteria. Cell 150, 606–619. [PubMed: 22819539]

Rathinam VAK, Zhao Y, and Shao F (2019). Innate immunity to intracellular LPS. Nat. Immunol 20, 527–533. [PubMed: 30962589]

Rühl S, and Broz P (2015). Caspase-11 activates a canonical NLRP3 inflammasome by promoting K(+) efflux. Eur. J. Immunol 45, 2927–2936. [PubMed: 26173909]

Russo AJ, Vasudevan SO, Méndez-Huergo SP, Kumari P, Menoret A, Duduskar S, Wang C, Sáez JMP, Fettis MM, Li C, et al. (2021). Intracellular immune sensing promotes inflammation via gasdermin D–driven release of a lectin alarmin. Nat. Immunol 22, 154–165. [PubMed: 33398185]

Schmid-Burgk JL, Gaidt MM, Schmidt T, Ebert TS, Bartok E, and Hornung V (2015). Caspase-4 mediates non-canonical activation of the NLRP3 inflammasome in human myeloid cells. Eur. J. Immunol 45, 2911–2917. [PubMed: 26174085]

Schromm AB, Brandenburg K, Rietschel E.Th., Flad H-D, Carroll SF, and Seydel U (1996). Lipopolysaccharide-binding protein mediates CD14-independent intercalation of lipopolysaccharide into phospholipid membranes. FEBS Lett 399, 267–271. [PubMed: 8985160]

Senatus L, López-Díez R, Egaña-Gorroño L, Liu J, Hu J, Daffu G, Li Q, Rahman K, Vengrenyuk Y, Barrett TJ, et al. (2020). RAGE impairs murine diabetic atherosclerosis regression and implicates IRF7 in macrophage inflammation and cholesterol metabolism. Jci Insight 5, e137289.

Shi J, Zhao Y, Wang Y, Gao W, Ding J, Li P, Hu L, and Shao F (2014). Inflammatory caspases are innate immune receptors for intracellular LPS. Nature 514, 187. [PubMed: 25119034]

Shi J, Zhao Y, Wang K, Shi X, Wang Y, Huang H, Zhuang Y, Cai T, Wang F, and Shao F (2015). Cleavage of GSDMD by inflammatory caspases determines pyroptotic cell death. Nature 526, 660–665. [PubMed: 26375003]

Tan Y, Zanoni I, Cullen TW, Goodman AL, and Kagan JC (2015). Mechanisms of toll-like receptor 4 endocytosis reveal a common immune-evasion strategy used by pathogenic and commensal bacteria. Immunity 43, 909–922. [PubMed: 26546281]

Vanaja SK, Russo AJ, Behl B, Banerjee I, Yankova M, Deshmukh SD, and Rathinam VAK (2016). Bacterial outer membrane vesicles mediate cytosolic localization of LPS and caspase-11 activation. Cell 165, 1106–1119. [PubMed: 27156449]

Wang H, Bloom O, Zhang M, Vishnubhakat JM, Ombrellino M, Che J, Frazier A, Yang H, Ivanova S, Borovikova L, et al. (1999). HMG-1 as a late mediator of endotoxin lethality in mice. Science 285, 248–251. [PubMed: 10398600]

Wright SD, Ramos RA, Tobias PS, Ulevitch RJ, and Mathison JC (1990). CD14, a receptor for complexes of lipopolysaccharide (LPS) and LPS binding protein. Science 249, 1431–1433. [PubMed: 1698311]

Wright SS, Vasudevan SO, and Rathinam VA (2021). Mechanisms and consequences of noncanonical inflammasome-mediated pyroptosis. J. Mol. Biol 434, 167245. [PubMed: 34537239]

Wu C, Lu W, Zhang Y, Zhang G, Shi X, Hisada Y, Grover SP, Zhang X, Li L, Xiang B, et al. (2019). Inflammasome activation triggers blood clotting and host death through pyroptosis. Immunity 50, 1401–1411.e4. [PubMed: 31076358]

Yang X, Cheng X, Tang Y, Qiu X, Wang Y, Kang H, Wu J, Wang Z, Liu Y, Chen F, et al. (2019). Bacterial endotoxin activates the coagulation cascade through gasdermin D-dependent phosphatidylserine exposure. Immunity 51, 983–996.e6. [PubMed: 31836429]

Youn JH, Oh YJ, Kim ES, Choi JE, and Shin J-S (2008). High mobility group box 1 protein binding to lipopolysaccharide facilitates transfer of lipopolysaccharide to CD14 and enhances lipopolysaccharide-mediated TNF-α production in human monocytes. J. Immunol 180, 5067–5074. [PubMed: 18354232]

Zanoni I, Ostuni R, Marek LR, Barresi S, Barbalat R, Barton GM, Granucci F, and Kagan JC (2011). CD14 controls the LPS-induced endocytosis of Toll-like receptor 4. Cell 147, 868–880. [PubMed: 22078883]

Zanoni I, Tan Y, Gioia MD, Springstead JR, and Kagan JC (2017). By capturing inflammatory lipids released from dying cells, the receptor CD14 induces inflammasome-dependent phagocyte hyperactivation. Immunity 47, 697–709.e3. [PubMed: 29045901]

Highlights

- CD14 is vital for cytosolic LPS sensing by the noncanonical inflammasome *in vivo*
- CD14 enables caspase-11 activation by facilitating the cytosolic transfer of LPS
- The role of CD14 in the cytosolic sensing of LPS is TLR4-independent

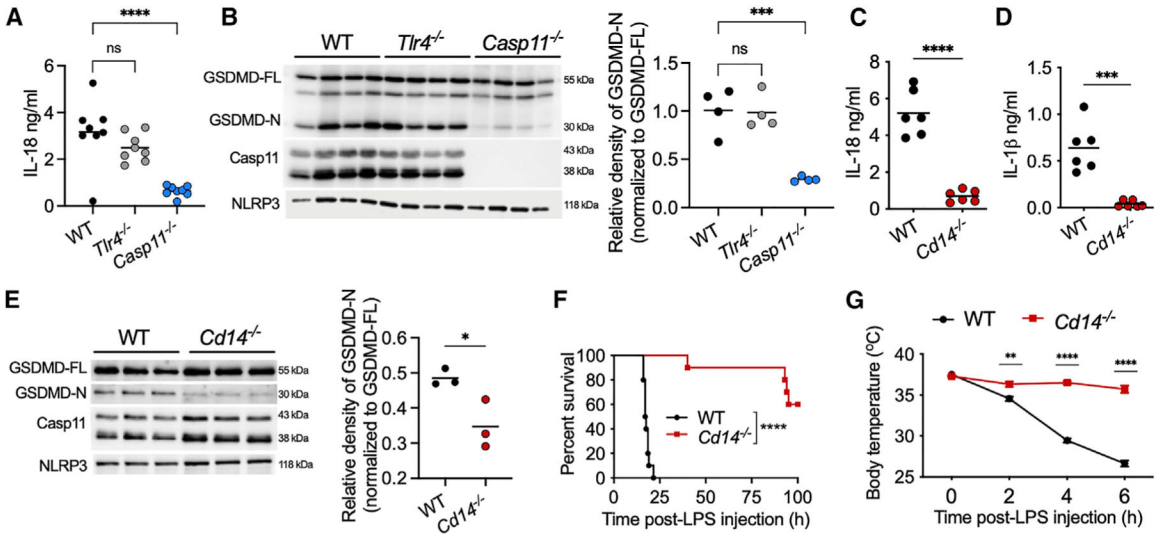

Figure 1. Noncanonical inflammasome activation by LPS *in vivo* is CD14-dependent

(A, C, and D) Plasma IL-18 (A and C) and IL-1β (D) in IFN-γ (1 μg; 3 h)-primed mice 6 h post-LPS (20 mg/kg) injection.

(B and E) Full-length and cleaved GSDMD (GSDMD-FL and GSDMD-N, respectively), caspase-11, and NLRP3 in spleen homogenates from indicated mice treated as above.

(F and G) Survival (F; n = 10 for each genotype) and body temperature (G; n = 10 for each genotype) of indicated mice primed with IFN-γ (0.25 μg; 3 h) and injected with LPS (10 mg/kg).

Data from two experiments (A, F, and G) or one experiment representative of two (B–E) are shown. Each circle represents a mouse, and horizontal lines represent mean (A–E). Data are presented as the mean ± SEM (G). *p < 0.05; **p < 0.01; ***p < 0.001; ****p < 0.0001; ns: non-significant; one-way ANOVA/Dunnett's test (A and B), unpaired two-tailed t test (C–E), Mantel-Cox test (F), or two-way ANOVA/Sidak's test (G).

See also Figure S1.

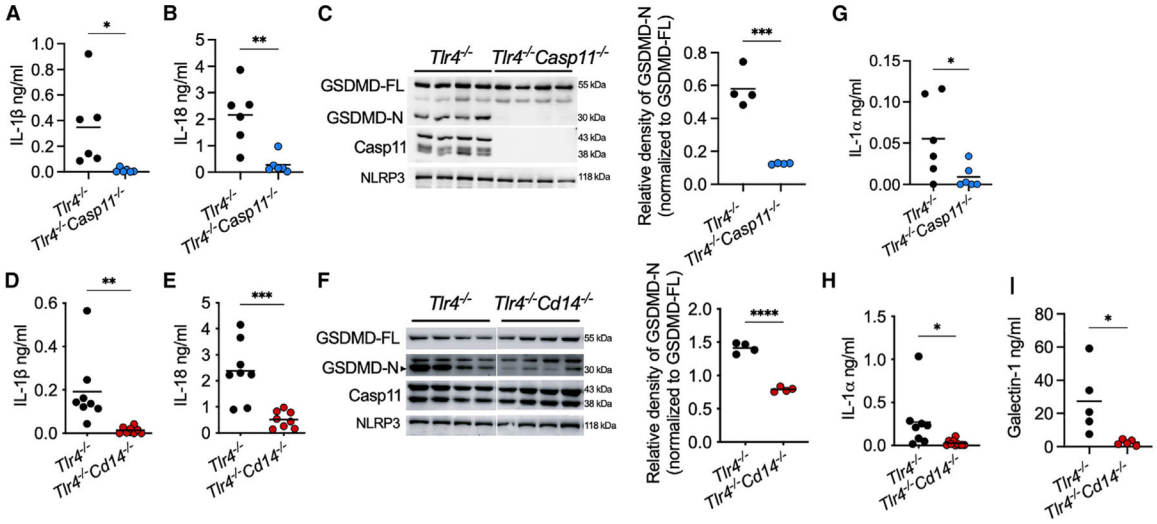

Figure 2. CD14 functions independent of TLR4 to activate the noncanonical inflammasome

(A, B, D, E, G, H, and I) Plasma IL-1β (A and D), IL-18 (B and E), IL-1α (G and H), and galectin-1 (I) in IFN-γ-primed mice 6 h post-LPS injection.

(C and F) GSDMD, caspase-11, and NLRP3 in spleen homogenates from indicated mice treated as above.

Data from two experiments (A, B, D, E, G, and H) or one experiment representative of two (C, F, and I) are shown. Each circle represents a mouse, and horizontal lines represent mean. *p < 0.05; **p < 0.01; ***p < 0.001; ****p < 0.0001; unpaired two-tailed t test.

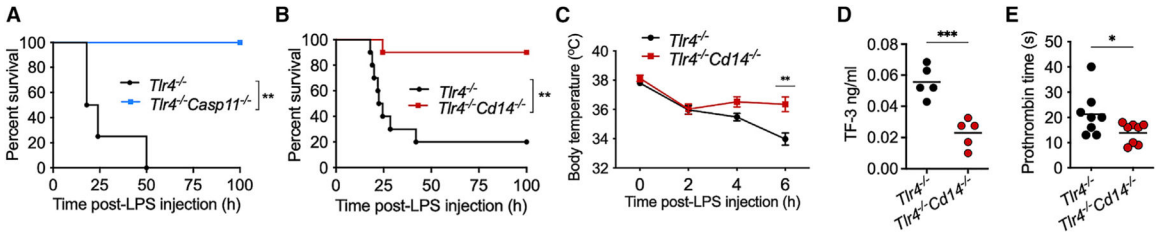

Figure 3. The contribution of CD14 to caspase-11-mediated lethal responses is TLR4-independent

(A and B) Survival of IFN-γ-primed LPS-injected *Tlr4*$^{-/-}$ (n = 5) and *Tlr4*$^{-/-}$ *Casp11*$^{-/-}$ (n = 5) (A) and *Tlr4*$^{-/-}$ (n = 10) and *Tlr4*$^{-/-}$ *Cd14*$^{-/-}$ (n = 10) (B) mice.

(C–E) Body temperature (n = 10) (C), plasma tissue factor-3 (TF-3) (D), and prothrombin clotting time (E) in *Tlr4*$^{-/-}$ and *Tlr4*$^{-/-}$ *Cd14*$^{-/-}$ mice treated as above. Data from two experiments (B–E) or one experiment (A) are shown. Data are presented as the mean ± SEM (C). Each circle represents a mouse, and horizontal lines represent mean (D and E). *p < 0.05; **p < 0.01; ***p < 0.001; Mantel-Cox test (A and B), two-way ANOVA/Sidak's test (C), or unpaired two-tailed t test (D and E).

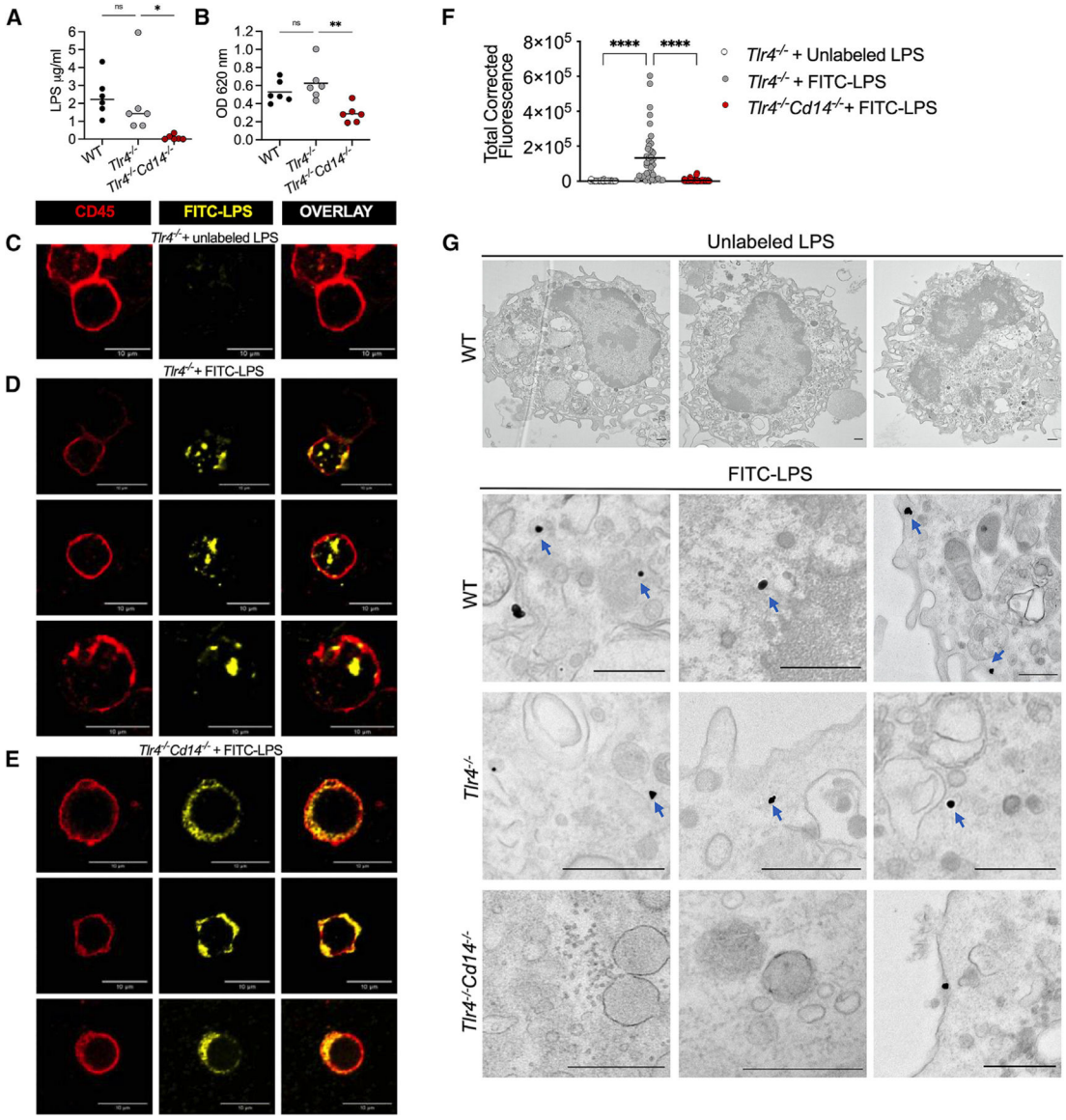

Figure 4. CD14 enables caspase-11 activation by facilitating intracellular LPS localization *in vivo*

(A and B) LPS levels in the splenic myeloid cell cytosol of WT, *Tlr4*$^{-/-}$, and *Tlr4*$^{-/-}$ *Cd14*$^{-/-}$ mice 5 h post-LPS injection assessed by the LAL (A) and HEK-TLR4 reporter cell (B) assays. Each circle represents a mouse, and horizontal lines represent mean.

(C–F) Confocal images of CD11b+ splenocytes sorted from unlabeled LPS-injected *Tlr4*$^{-/-}$ mice (C) or FITC-LPS-injected *Tlr4*$^{-/-}$ (D) and *Tlr4*$^{-/-}$ *Cd14*$^{-/-}$ (E) mice and stained with anti-FITC and anti-CD45 antibodies and the quantification of intracellular FITC-LPS intensity (F) (each circle represents a cell and horizontal lines represent mean).

(G) EM images of peritoneal lavage cells from indicated mice injected with unlabeled or FITC-labeled LPS and stained with anti-FITC gold particles. Blue arrows indicate cytosolic localization of LPS.

Data from five experiments (A and B), representative images (C–E) from four experiments, combined data (F) from four experiments, and representative images from three experiments

(G) are shown. *p < 0.05; **p < 0.01; ****p < 0.0001; ns: non-significant; one-way ANOVA/Dunnett's test. Scale bar: 10 μM (C–E) or 0.5 μM (G).
See also Figures S2, S3, and S4.

KEY RESOURCES TABLE

REAGENT or RESOURCE	SOURCE	IDENTIFIER
Antibodies		
Rabbit monoclonal anti-human/mouse NLRP3 (Clone D4D8T)	Cell Signaling Technology	Cat# 15101; RRID:AB_2722591
Rabbit monoclonal anti-mouse GSDMD (Clone EPR 19828)	Abcam	Cat# Ab209845; RRID:AB_2783550
Rat monoclonal anti-mouse Caspase 11 (Clone 17D9)	Cell Signaling Technology	Cat# 14340S; RRID:AB_2728693
Anti-Rat IgG HRP	Jackson ImmunoResearch Labs	Cat# 712-035-150; RRID:AB_2340638
Anti-Rabbit IgG HRP	Jackson ImmunoResearch Labs	Cat# 711-035-152; RRID:AB_10015282
Rat monoclonal anti-IL-18 antibody (Clone 74; ELISA capture antibody)	MBL International	Cat# D047-3; RRID:AB_592016
Rat monoclonal anti-IL-18 antibody Biotin (Clone 93-10C; ELISA detection antibody)	MBL International	Cat# D048-6; RRID:AB_592012
APC-anti-mouse/human CD11b antibody (Clone M1/70)	BioLegend	Cat# 101212; RRID:AB_312795
FITC-anti-mouse/human CD11b antibody (Clone M1/70)	BioLegend	Cat# 101206; RRID:AB_312789
Monoclonal mouse anti-fluorescein (FITC) antibody (Clone 1F8.1E4)	Biotium	Cat# 20210
APC-anti-mouse CD45.2 antibody (Clone 104)	Invitrogen	Cat# 17-0454-82
Rabbit monoclonal anti-human/mouse/rat EEA1 (Clone 45B10)	Cell Signaling Technology	Cat# 3288S; RRID:AB_2096811
Rat monoclonal anti-mouse CD107a (Lamp1) (Clone eBio1D4B)	eBioscience	Cat# 14-1071-85; RRID:AB_657533
APC-anti-mouse CD14 (Clone Sa2-8)	Invitrogen	Cat# 17-0141-81; RRID:AB_469352
Rabbit polyclonal anti-human/mouse/rat Galectin-3 (Clone D4I2R)	Cell Signaling Technology	Cat# 12733; RRID:AB_2798009
Mouse monoclonal Rab5A (Clone E6N8S)	Cell Signaling Technology	Cat# 46449S; RRID:AB_2799303
CF405M-Goat anti-rat IgG (H+L)	Biotium	Cat# 20374
CF405M-Goat anti-rabbit IgG (H+L)	Biotium	Cat# 20373
CF647-Goat anti-rabbit IgG (H+L)	Biotium	Cat# 20282; RRID:AB_10853478
Mouse monoclonal anti-FITC gold conjugate	Electron Microscopy Sciences	Cat# 25581
Chemicals, peptides, and recombinant proteins		
LPS E. *coli* O111:B4	Sigma	Cat# L3024-25MG
FITC-conjugated LPS *E. coli* O111:B4	Sigma	Cat# F3665-10MG
Recombinant mouse IFN-γ	R&D Systems	Cat# 485-MI-100
Collagenase	Sigma Aldrich	Cat# C5138-5G
DNase I	Sigma Aldrich	Cat# DN25-1G
Recombinant mouse IL-18 (ELISA standard)	MBL	Cat# B002-5
Pam3CSK4	InvivoGen	Cat# tlrl-pms
Recombinant HMGB1	HMGBiotech	Cat# HM-114
RAGE inhibitor FPS-ZM1	Cayman	Cat# 11909
RAGE Antagonist Peptide (RAP)	Millipore	Cat# 553031
Critical commercial assays		
Mouse IL-1β ELISA kit	Thermo Fisher Scientific	Cat# 50-171-85
Mouse TNF ELISA kit	Thermo Fisher Scientific	Cat# 88-7324
Mouse IL-1α ELISA kit	Thermo Fisher Scientific	Cat# 88-5019

REAGENT or RESOURCE	SOURCE	IDENTIFIER
Mouse Galectin-1 ELISA kit	R&D Systems	Cat# DY1245
Pierce™ BCA Protein Assay kit	Thermo Fisher Scientific	Cat# 23227
Halt™ Protease Inhibitor Cocktail (100X)	Thermo Fisher Scientific	Cat# 1861279
NuPAGE LDS sample buffer (4X)	Invitrogen	Cat# NP0007
Trans-Blot Turbo Transfer System	Bio-Rad	Cat# 1704271
Clarity ECL HRP Substrate	Bio-Rad	Cat# 170-5060S
Mouse Coagulation Factor III/TF ELISA kit	R&D systems	Cat# DY3178-05
Pacific Hemostasis Thromboplastin-D	Thermo Scientific	Cat# 100356TS
ACK Lysis buffer	Gibco	Cat# A1049201
Chromo-LAL	Associates of Cape Cod	Cat# C0031-5
Glucashield® (1→3)-ß-D-Glucan Inhibiting Buffer	Associates of Cape Cod	Cat# GB051-5
HEK-Blue Detection	Invivogen	Cat# hb-det2
HEK-Blue Selection	Invivogen	Cat# hb-sel
Lipofectamine 2000	Invitrogen	Cat# 11668027
GoldEnhance EM kit	Nanoprobes	Cat# 2113-8ML
Experimental Models: Cell lines		
HEK-Blue™ hTLR4	InvivoGen	Cat# hkb-htlr4
Experimental models: Organisms/strains		
Mouse: C57BL/6J	The Jackson Laboratory	RRID:IMSR_JAX:000664
Mouse: *Casp11*$^{-/-}$	Kayagaki et al., Nature 2011 Genentech	N/A
Mouse: *Tlr4*$^{-/-}$	The Jackson Laboratory	RRID:IMSR_JAX:007227
Mouse: Cd14$^{-/-}$	The Jackson Laboratory	RRID:IMSR_JAX:003726
Mouse: *Tlr4*$^{-/-}$ *Cd14*$^{-/-}$	Generated in this study	N/A
Mouse: *Tlr4*$^{-/-}$ *Casp11*$^{-/-}$	Generated in this study	N/A
Oligonucleotides		
Casp11$^{-/-}$ genotyping Primer 1: CCCTGGAAAAATCGATGACT	Kayagaki et al., Nature 2011 & Integrated DNA Technologies	Mouse listed above
Casp11$^{-/-}$ genotyping Primer 2: TGAAATGCATGTACTGAGAGCAAGG	Kayagaki et al., Nature 2011 & Integrated DNA Technologies	Mouse listed above
Casp11$^{-/-}$ genotyping Primer 3: CAATTGACTTGGGGATTCTGG	Kayagaki et al., Nature 2011 & Integrated DNA Technologies	Mouse listed above
Tlr4$^{-/-}$ genotyping Primer 1 oIMR8365: GCAAGTTTCTATATGCATTCTC	The Jackson Laboratory & Integrated DNA Technologies	Mouse listed above
Tlr4$^{-/-}$ genotyping Primer 2 oIMR8366: CCTCCATTTCCAATAGGTAG	The Jackson Laboratory & Integrated DNA Technologies	Mouse listed above
Tlr4$^{-/-}$ genotyping Primer 3 oIMR8367: TATGCATGATCAACACCACAG	The Jackson Laboratory & Integrated DNA Technologies	Mouse listed above
Tlr4$^{-/-}$ genotyping Primer 4 oIMR8368: TTTCCATTGCTGCCCTATAG	The Jackson Laboratory & Integrated DNA Technologies	Mouse listed above
Cd14$^{-/-}$ genotyping Primer 1 oIMR0662: CCGCTTCCATTGCTCAGCGG	The Jackson Laboratory & Integrated DNA Technologies	Mouse listed above
Cd14$^{-/-}$ genotyping Primer 2 oIMR1314: CCAAGTTTTAGCGCTGCGTAAC	The Jackson Laboratory & Integrated DNA Technologies	Mouse listed above
Cd14$^{-/-}$ genotyping Primer 3 oIMR1315: GCCAGCCAAGGATACATAGCC	The Jackson Laboratory & Integrated DNA Technologies	Mouse listed above

REAGENT or RESOURCE	SOURCE	IDENTIFIER
Software and Algorithms		
GraphPad Prism 9.3	GraphPad Software	N/A
Fiji/ImageJ (version 10.2)	https://imagej.net/Fiji	N/A